

## The Calibration and Intercalibration of Sea-Going Infrared Radiometer Systems Using a Low Cost Blackbody Cavity

C. J. DONLON\*

*Southampton Oceanography Centre, University of Southampton, Southampton, United Kingdom*

T. NIGHTINGALE

*Rutherford Appleton Laboratory, Oxford, United Kingdom*

L. FIEDLER

*Max-Planck-Institut für Meteorologie, Hamburg, Germany*

G. FISHER, D. BALDWIN, AND I. S. ROBINSON

*Southampton Oceanography Centre, University of Southampton, Southampton, United Kingdom*

(Manuscript received 10 January 1998, in final form 28 August 1998)

### ABSTRACT

There are many infrared radiometer systems available for the measurement of in situ sea surface skin temperature (SSST). Unfortunately, the marine environment is extremely hostile to optical components, and to ensure the accuracy of SSST measurements, an absolute calibration of instrumentation using an independent calibration reference is required both before and after any sea deployment. During extended deployments it is prudent to have additional regular calibration data to monitor instrument performance characteristics. This paper presents a design for an ambient temperature (278–325 K), wide aperture (100 mm), reference blackbody unit that may be used to calibrate a variety of sea-going infrared radiometer systems both in the laboratory and in the field. The blackbody consists of a spun copper cavity coated with well-characterized high emissivity paint (Mankiewicz Nextel Velvet Coating 811-21) immersed in a water bath that is continuously mixed using a strong water pump. The radiant temperature of the blackbody cavity is determined from the measured water bath temperature. Results derived from validation and intercomparison experiments show this blackbody design to be an accurate and reliable reference blackbody source. However, in order to ensure that the best possible calibration data are obtained, extreme care must be taken to ensure the accurate measurement of the water bath temperature, proper positioning of a radiometer in front of the cavity itself, and prevention of condensation on the cavity surface. Four blackbody units have been specifically built for the European Union combined action for the study of the ocean thermal skin (CASOTS) program. Using these units as reference radiance sources, the authors describe the strategy adopted and present results obtained from the CASOTS radiometer intercalibration experiment. These results highlight the need to obtain independent calibration data both before and after sea-going radiometer deployments and the need to standardize field radiometer calibration protocols.

### 1. Introduction

There are many groups currently involved in the in situ measurement of radiometric sea surface skin temperature (SSST) from ships (e.g., Schlüssel et al. 1987,

1990; Kent et al. 1996; Donlon and Robinson 1997) and aircraft (e.g., Smith et al. 1994). These measurements are used to investigate the bulk skin sea surface temperature difference  $\Delta T$  and validate satellite SSST observations (e.g., Thomas and Turner 1995; Donlon and Robinson 1998). Currently, a wide variety of infrared radiometer systems are used to determine the in situ SSST, although no standard instrument calibration procedure or deployment protocols have been established. Unfortunately, the marine environment is extremely hostile to radiometer systems and the effects of saline aerosol could severely degrade instrument fore-optics and internal calibration reference cavities. To monitor such degradation both pre- and postdeployment cali-

---

\* Current affiliation: Space Applications Institute, Marine Environment Unit, Joint Research Centre, Ispra, Italy.

---

Corresponding author address: Dr. Craig J. Donlon, CEC-JRC ISPRA, Space Applications Institute, Marine Environment Unit, I-21020 Ispra, Italy TP690.  
E-mail: craig.donlon@jrc.it

bration data should be obtained across the range of SSST encountered during a deployment, using an independent reference radiance source. In order to address many of these issues a concerted action project was initiated within the European Union Environment and Climate Programme. Entitled “Combined action for the study of the ocean thermal skin” (CASOTS), it included an SSST radiometer intercalibration experiment designed to verify and intercompare the performance of several radiometer systems used by different research groups. In particular it aimed to establish the collective degree of scatter when all radiometer systems were compared to a reference radiance source maintained at different temperatures over the range of global SSST. This exercise was repeated in a number of different temperature environments simulating the typical temperature conditions of tropical, midlatitude, and high latitude regions. The purpose of this activity was to promote the intercalibration of sea-going infrared radiometers using a reference radiance source that is relatively inexpensive and easily replicated.

This paper is split into two broad sections, where the first part describes in detail the calibration radiance targets specifically developed for the first CASOTS workshop. The second part then focuses on the experimental design, implementation, and results obtained from the CASOTS radiometer intercalibration experiment.

## 2. Specification for a blackbody cavity to calibrate infrared radiometers

To fundamentally calibrate a radiometer, a well-defined calibration radiance target, which entirely fills the radiometer field of view, is required to derive an appropriate radiance-to-temperature relationship accounting for the specific spectral characteristics of the particular radiometer. Denoting the Planck function as  $B(T, \lambda)$ , which describes the radiance at wavelength  $\lambda$  emanating from a blackbody target source at temperature  $T$ , if we consider a radiometer viewing a target source at a temperature  $T_a$  and emittance  $\epsilon_\lambda$ , the measured signal  $S_a$  is given by

$$S_a = \int_0^\infty \phi_\lambda [\epsilon_\lambda B(T_a, \lambda) + (1 - \epsilon_\lambda) B(T_e, \lambda)] d\lambda, \quad (1)$$

where  $B(T_e, \lambda)$  is the radiance emanating from the surrounding environment at temperature  $T_e$ , and  $\phi_\lambda$  is the spectral response of the particular radiometer. For an ideal blackbody target (i.e.,  $\epsilon_\lambda = 1$ ), Eq. (1) reduces to

$$S_a(T_i) = \int_0^\infty \phi_\lambda B(T_i, \lambda) d\lambda, \quad (2)$$

in which  $T_i$  is the the equivalent blackbody temperature or brightness temperature.

Grassl and Hinzpeter (1975) describe a calibration strategy developed to maintain the calibration of infra-

red radiometers commonly referred to as the “stirred tank” calibration. This has been used by several authors to verify the accuracy of several sea-going radiometer systems (e.g., Thomas and Turner 1995; Kent et al. 1996) or to operationally calibrate sea-going infrared radiometers (e.g., Saurez et al. 1997; Schlüssel et al. 1990). In this scheme, a radiometer periodically views (typically once per minute) a vigorously stirred bath of seawater. The temperature of the water bath is accurately measured and, assuming that stirring prevents any vertical or horizontal temperature gradients (including a skin temperature deviation) and that the environmental conditions (e.g., cloud cover and wind speed) remain constant throughout the calibration interval, the water bath can be considered as a calibration radiance source of known temperature. The radiometer signal is absolutely calibrated by relating the measured water bath temperature to the radiometer signal. One of the major benefits of this strategy when measuring SSST is that, if seawater is used in the calibration bath, the seawater emissivity term is eliminated from both the calibration exercise and seawater measurements. However, a major assumption is that the different surface roughness characteristics of the sea surface and water bath are equal.

Many bucket stirring systems use a vertical jet of water to mix the surface, which often results in a small bulge of water at the bucket center. Fiedler and Bakan (1997) describe how such a feature changes the angle of incidence of emitted and reflected radiation of the bucket relative to the sea surface, noting that on average, the angle is reduced, resulting in a slightly higher surface emissivity for the water in the bucket. Zappa (1997) used precision thermal imagery to validate the stirred bath calibration method and show that the effect of “wind” gusts blowing over the surface of the stirred bath can introduce a cool bias of  $\sim 0.1$  K to the calibration process for typical ocean-atmosphere conditions. Experiments using interferometric measurements of a stirred bucket calibration system (Fiedler and Bakan 1997) also find that a skin temperature deviation persists at the water surface relative to a 10-mm temperature measurement, having a magnitude of  $-1.2 \pm 0.07$  K. In order to reduce this bias, the surface renewal times within the stirred tank must be vigorous enough to offset the cooling effect of an increased heat flux out of the bath forced by wind gusts. This requires more intensive stirring, which in turn results in a larger water bulge on the water bath surface, exacerbating the problem. We note that nonvertical or diffused pumping systems may help to eliminate the water bulge and minimize this effect although such systems have not been widely used. Finally, the practical difficulties of operating a bucket system at sea include the complexity of mounting the often cumbersome bucket system (e.g., Saurez et al. 1997), the provision of a dedicated and continuous supply of seawater and power to the bucket system, and preventing water spray from contaminating the radiometer fore-optics. In our experience, most of the con-

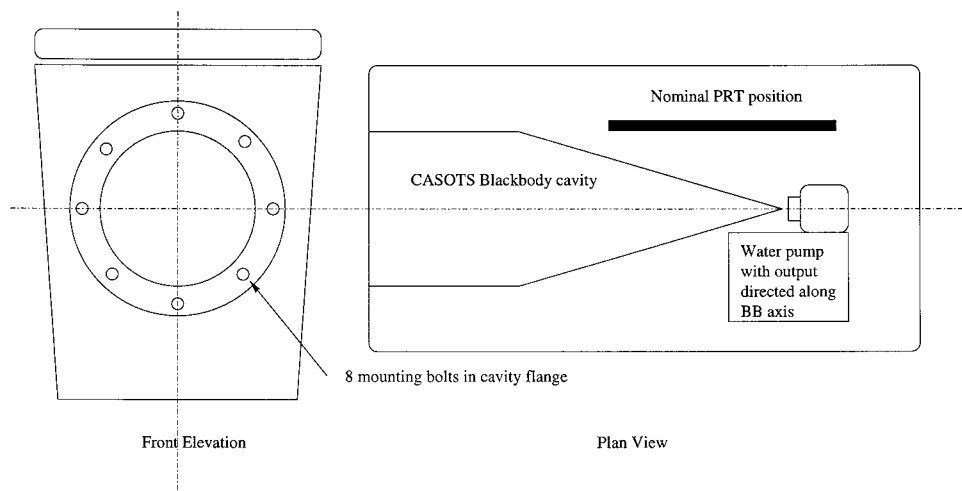


FIG. 1. A schematic diagram showing the general layout of the CASOTS blackbody unit. The relative positions of the blackbody cavity, a nominal PRT, and the water pump are shown. The water bath is approximately  $70 \times 30 \times 30$  cm.

tamination originates as spray from the bucket itself, which often results in the instrument fore-optics becoming completely wet. In this case, the radiometer will be unable to measure SSST but rather the temperature of the thin water film on the instrument fore-optics due to the high emissivity of water at the wavelengths of interest ( $10\text{--}12\ \mu\text{m}$ ).

We prefer a different approach to ship radiometer calibration, which relies on presenting a fabricated blackbody cavity of known emissivity and temperature to the radiometer as a calibrated radiance source. The critical elements of such a blackbody design are summarized by the following specifications.

- The aperture of the cavity should be large enough to accommodate radiometer systems having strongly divergent (up to  $15^\circ$ ) fields of view at 100 mm in front of the blackbody (BB) aperture.
- The operating temperature range of the cavity should include the range of expected global SSST ( $273\text{--}323$  K).
- The cavity should have a well-defined emissivity ( $\epsilon$ ) value greater than 0.99 for the  $8\text{--}14\text{-}\mu\text{m}$  spectral wave band.
- The temperature of the cavity should be accurately determined to  $\pm 0.05$  K from simple but reliable measurements.
- Temperature gradients within the cavity should be negligible ( $< 1.0\ \text{K m}^{-1}$ ).
- The unit should be portable and capable of operation in the most basic “laboratory” conditions, typical of research cruise situations.

These requirements can be fulfilled by a blackbody cavity, which is immersed in a well-stirred, temperature-controlled water bath following the basic design philosophy of Geist and Fowler (1986). The assumption is made that if the water bath is adequately mixed, tem-

perature gradients within the bath and along the blackbody cavity walls can be maintained at a very low value apart from the region immediately close to the cavity aperture where strong gradients will persist because of mounting flanges and incomplete thermal coupling to the water bath. With this design, an accurate water temperature measurement will then be sufficient to define the temperature of the radiating cavity. We modify the basic design of Geist and Fowler (1986) because its large size is unsuitable for portable use.

A schematic sketch of the completed CASOTS BB is given in Fig. 1. The unit consists of a blackbody cavity which is mounted within a water bath and a strong water pump to mix the water within the bath. A precision platinum resistance thermometer (PRT) sensor is nominally shown mounted using adjustable clamps allowing the position of the sensors to be changed relative to the blackbody cavity. As there are a wide variety of configurations and sensor systems available to monitor the temperature of the CASOTS BB water bath, we will only discuss the specific thermometry systems used in the experiments reported here.

#### a. Blackbody cavity design

We require a diffuse surface finish for the cavity as this will be less sensitive to slight contamination when compared to a specular surface finish. Mankiewicz Nextel Velvet Coating 811-21 paint<sup>1</sup> was chosen for this purpose, which is a highly diffuse paint, originally developed by the 3M Company (Betts et al. 1985). More recently the formulation has been acquired and devel-

<sup>1</sup> Available from Mankiewicz Gebr. and Co., Georg-Wilhelm-Strasse 189, D-21107 Hamburg, Germany.

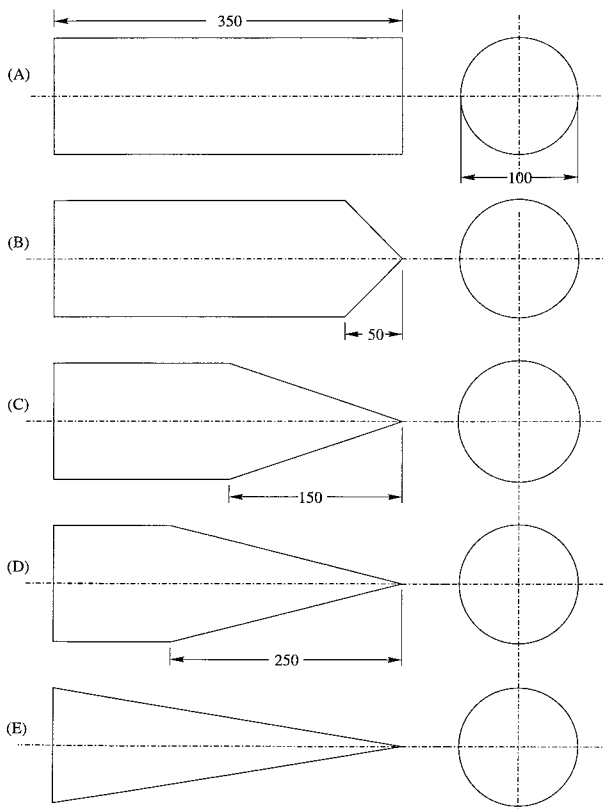


FIG. 2. Specific blackbody cavity designs considered during the development of the CASOTS blackbody cavity.

oped by Mankiewicz and no longer shows the dip in emissivity at  $9 \mu\text{m}$  characteristic of its predecessor. Nextel Velvet Coating 811-21 has a measured  $\epsilon$  of 0.97 or better throughout the spectral range  $5\text{--}35 \mu\text{m}$  (Lohrenge and Todtenhaupt 1996).

The emissivity of a blackbody cavity is determined by its geometry as well as its surface finish. Repeated internal reflections multiply the emissivity of the surface coating, and by a prudent choice of shape, the effective emissivity of the cavity can be increased many times. Berry (1981) prefers a geometry incorporating a reentrant cone at the base of the blackbody and a restricted aperture but, due to the need for a large aperture and a straightforward construction technique, we consider a few simple combinations of cones and cylinders. These are shown in Fig. 2.

The effective emissivity was calculated for each geometry as a function of the “spot” radius of a radiometer field of view falling on the deepest part of the cavity by an extension of the net radiation method (Siegel and Howell 1981; Nightingale 1992). The results are plotted in Fig. 3 using a conservative estimate of  $\epsilon = 0.96$  for the emissivity of the Nextel paint. We choose  $\epsilon = 0.96$  to account for inevitable imperfections in the paint finish. The effective emissivity of the simple cylindrical flat-bottomed pot shown in Fig. 3a is almost

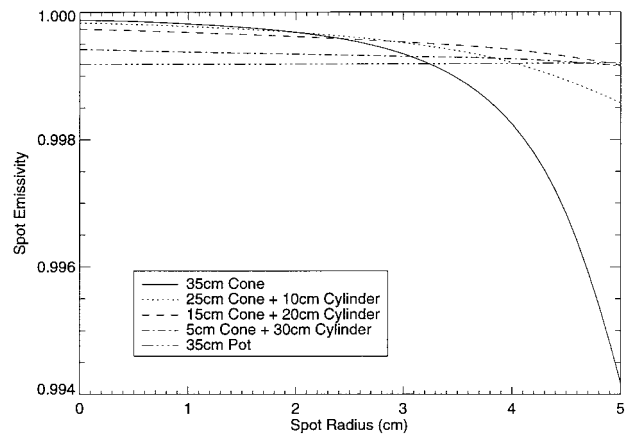


FIG. 3. Effective emissivities of the blackbody cavity geometries shown in Fig. 2, calculated as a function of the spot radius of a radiometer view to the center of the cavity, for a diffuse surface emissivity of 0.96.

invariant with spot radius, as the view factor from the flat base to the aperture changes very little with radius. However, as the base is parallel to the aperture, these factors are relatively large, giving a poor peak emissivity.

The simple cone shown in Fig. 3e has a very high emissivity at small spot radii as the observed surface is oblique to all parts of the aperture and deeply buried. However, as the spot radius increases much of the observed surface moves nearer to the aperture. The surface is increasingly exposed to the aperture and the emissivity value decreases rapidly. The performance of the simple cone steadily deteriorates as the spot radius increases beyond 25 mm compared with the other geometries shown in Fig. 3.

A good compromise can be found between these extremes. Hybrids of the pot and cone schemes have high effective emissivities for a large range of spot radii, an essential requirement if the blackbody is to be applicable to a wide range of radiometers. The design shown in Fig. 3d was finally chosen for its high emissivity at radii up to 40 mm and its relative ease of construction and coating. Each cavity was spun over a steel mandrel from a single sheet of copper, giving an extremely sharp apex. However, to ensure that no specular reflections resulted from within the very tip of the cone (due to incomplete paint coverage), the lower 25 mm of the cone was offset  $\sim 2^\circ$  from the central axis of the cavity after the cone had been fabricated.

#### b. Blackbody cavity temperature regulation

Although Peltier cooling devices were considered as a means to control the temperature of the cavity, the simplicity and robustness of a well-stirred water jacket together with the relative ease of temperature measurement using immersible sensors is a much more attractive solution. The water bath was adapted from a high in-



sulation rectangular commercial “cool box” and fitted with a large volume reduction water pump (flow rate of  $46 \text{ L min}^{-1}$ ) having a directional output. An induction water pump was originally chosen because such devices have all electrical circuitry potted into a waterproof block, although several other designs have subsequently been used. Following Geist and Fowler (1986), we direct the water output from the pump along the cone axis to ensure an isothermal cavity temperature. The temperature of the CASOTS BB can then be simply controlled by adding hot or cold water to the water bath and allowing a stabilization time lag of typically 30–60 s to ensure complete mixing. The preferable method is to use a small immersible heater system to gradually raise the water bath temperature. Commercial aquarium heaters offer a satisfactory solution for this purpose. To include a temperature regulation system that would maintain the water bath at a constant temperature (not a design requirement for the CASOTS BB) requires a significant increase in the size, complexity, and weight of the CASOTS BB, resulting in a nonportable device. Even if such controlling systems are included, a suitable stabilization time is still required for the system to reach a desired precision because of the inherent hysteresis in the temperature regulation systems as discussed by Bell (1995) and Geist and Fowler (1986). We note here that for special circumstances, such as operating in an aircraft environment, significant changes to the water bath design would be required.

### 3. Performance of the CASOTS blackbody

In order to discuss the performance of the CASOTS BB design, a series of experiments were undertaken using a variety of radiometer instruments, temperature sensors, and intercomparison techniques described below.

#### a. Temperature gradients across the CASOTS blackbody

Incomplete stirring of the water bath will result in significant temperature gradients within the CASOTS BB cavity. To investigate this possibility, a Raytheon MWIR HS thermal camera was used to obtain a number of thermal images of the CASOTS BB cavity. The camera has a spectral range of  $3\text{--}5 \mu\text{m}$  and uses a Stirling cycle cooler to actively cool a  $256 \times 256$  InSb detector array and maintain a noise equivalent difference temperature of  $<0.025 \text{ K}$  at  $296 \text{ K}$ . Figure 4 shows a typical example thermal image of the CASOTS BB cavity aperture obtained using the MWIR camera. The mean temperature across the image is  $300 \text{ K}$  and the ambient room temperature was  $\sim 297 \text{ K}$ . The grayscale color table has been stretched so that the range of temperatures shown spans the range  $300\text{--}300.15 \text{ K}$  and the standard deviation across the image is  $0.02 \text{ K}$ . These data clearly demonstrate that thermal gradients within the cavity are

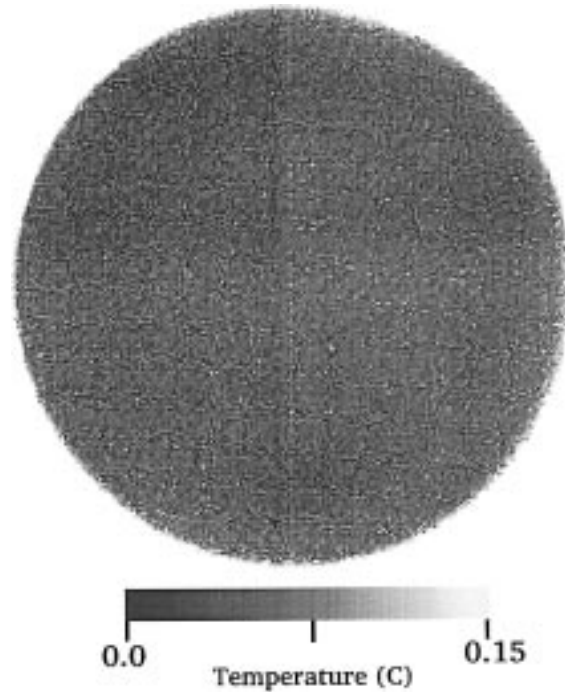


FIG. 4. Thermal image of CASOTS-002 blackbody taken using a Raytheon MWIR HS thermal camera. For this particular image, the mean temperature across the CASOTS cavity of  $300 \text{ K}$  has been subtracted from the data and a spot diameter of  $80 \text{ mm}$  has been overlaid for reference. The standard deviation of this image is  $0.02 \text{ K}$ . The camera has a spectral waveband of  $3\text{--}5 \mu\text{m}$  and a noise equivalent difference temperature of  $<0.025 \text{ K}$  at  $296 \text{ K}$ . At the time of image acquisition, the ambient room temperature was  $297 \text{ K}$ .

minimal for a radiometer spot radius of  $<40 \text{ mm}$ . A significant temperature deviation ( $>0.5 \text{ K}$ ) is characteristic of the cavity aperture and mounting flange (spot radii of  $40\text{--}50 \text{ mm}$ ) because the cavity flange and first  $20 \text{ mm}$  of the cylindrical cavity wall are only in contact with the water bath wall and not the water held within. A time series of these data when displayed as an animated movie show that random, small ( $\text{mm}$ ), and transient ( $<3 \text{ s}$ ) thermal features are apparent along the CASOTS BB, which are associated with the mixing characteristics of the water bath and pump arrangement.

Based on the results of our theoretical calculations shown in Fig. 3, we recommend that a radiometer spot radius should not exceed  $40 \text{ mm}$  if the mounting flange effects described above are to be avoided and no correction for the nonunity value of the cavity emissivity is to be made. External reflection effects could be minimized by using an end plate to limit the blackbody aperture, thus increasing the number of internal reflections as suggested by Berry (1981). However, an end plate baffle would restrict the aperture size of the CASOTS BB and would need to be tailored to a particular radiometer instrument. Consequently, we do not discuss this any further.

### b. Temperature drift of the CASOTS blackbody

As the CASOTS BB design does not use any form of thermostatic temperature regulation, there is potential for the cavity temperature to substantially drift due to heat loss via the cavity walls, water surface, and warming by the water pump.<sup>2</sup> We emphasize that the CASOTS BB is not designed to maintain a steady radiant temperature, but rather to provide a range of values that can be used to provide a comprehensive calibration of a particular radiometer. In this sense, the cavity temperature drifts slowly enough so that adequate measurements can be obtained by a radiometer to derive a robust calibration. The use of a large water bath, the small heating effect of the water pump, together with thermally insulated walls means that there is a substantial buffer of heat available to stabilize conduction across the blackbody cavity wall. In practice, experiments demonstrated that only when the cavity temperature was significantly different from the ambient air temperature were noticeable temperature drifts found.

The greatest drifts in cavity temperature are always when the water bath is operated with the cover open allowing direct heat exchange across the air–water interface of the bath. The temperature drift is always substantially less when the water bath cover is closed. To demonstrate a typical magnitude for a “worst case” cavity temperature drift of the CASOTS BB, we use data obtained from calibration experiments made during the Third Atlantic Meridional Transect (ROSSA/AMT-3) experiment (Donlon 1997). A CASOTS BB was used to calibrate a scanning infrared sea surface temperature radiometer (SISTeR). The SISTeR is a compact and flexible chopped, self-calibrating infrared filter radiometer, containing filters centered at 3.7, 10.8, and 12.0  $\mu\text{m}$ . A scan mirror selects between instrument views to the exterior and to two internal blackbodies. One is operated at ambient temperature and the other at a programmable increment (typically 10 K) above this. Each blackbody contains an embedded rhodium iron thermometer and is calibrated completely against a standard thermometer, traceable to the U.K. National Physical Laboratory realization of the ITS-90 temperature scale. Calibration data were obtained at 10-min intervals with the water bath cover open. The ambient temperature remained at  $293 \pm 0.5$  K throughout the calibration. The temperature difference between the ambient temperature and CASOTS BB temperature for a 3-h period has been plotted as a function of the temperature drift of the CASOTS BB, and is shown in Fig. 5. The temperature drift of the CASOTS BB is small and linearly related to the difference between the ambient air temperature and the CASOTS BB temperature. The drift rate is minimal at

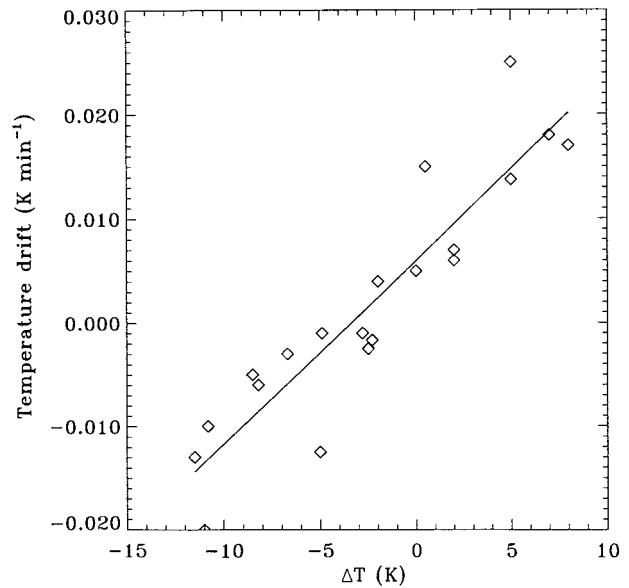


FIG. 5. The difference between CASOTS BB temperature and air temperature plotted as a function of the CASOTS BB temperature drift. Temperatures were logged by digital SIS thermometers calibrated to an accuracy of  $\pm 0.002$  K during the ROSSA-AMT-3 experiment.

ambient temperature and increases in magnitude as the ambient–BB temperature difference increases. Even at large ambient–BB temperature differences (e.g.,  $>10$  K), the temporal drift is small ( $<0.03$  K  $\text{min}^{-1}$ ). Given that most radiometers have a time constant on the order of several seconds, such a small value can be considered negligible. However, for completeness, the following polynomial equation describes the fitted line shown in Fig. 5, which can be used to facilitate a correction for this effect when the water bath cover is not used (the effect is negligible when the bath cover is used):

$$D = 5.9 \times 10^{-3} + (T_A - T_B)(1.8 \times 10^{-3}), \quad (3)$$

where  $D$  is the temperature drift (K  $\text{min}^{-1}$ ) of the CASOTS BB referenced to a temperature of 293 K,  $T_A$  is the ambient air temperature, and  $T_B$  is the temperature of the CASOTS BB.

### c. Cross calibration of the CASOTS BB using independent measurements

In order to verify the absolute accuracy of the CASOTS BB units, an independent measure of the CASOTS BB is required for a range of temperatures. One common method adopted for this purpose is to derive temperatures from a radiometer alternately viewing the CASOTS BB and a second independent blackbody unit maintained at similar temperatures. Assuming the radiometer is stable over the time period required to measure the temperature of each BB unit, the difference between the radiometer temperature and the BB temperature should be the same for each blackbody within

<sup>2</sup> Experience shows that warming by the water pump is a viable means to very slowly (5–6 h) raise the temperature of the CASOTS BB, providing a range of radiant temperatures.

the uncertainty of both the radiometer and BB temperature measurements.

#### COMPARISON BETWEEN THE CASOTS BB AND AN EPPLEY BB25TB BLACKBODY

Radiant temperatures were derived from measurements made by two TASCOTHI-500L radiometers alternately viewing a CASOTS BB and a second variable temperature blackbody in a stable temperature room. An Eppley blackbody (Model BB25TB 10194) was used as an independent blackbody unit, which uses a combination of thermoelectric heat pumping and forced convective heat sink cooling to vary the temperature of a copper baseplate that is attached to a copper hexagonal cavity array (honeycomb) coated with Chemglaze Z306 high emissivity paint. A single PRT sensor is mounted within the copper plate to determine the radiant temperature of the blackbody cavity, which has a source area of  $250 \times 250$  mm (although the view port is  $\sim 50 \times 50$  mm). The emissivity of the cavity is quoted to be better than 0.995, having a temperature uniformity and stability  $\pm 0.1$  K and an accuracy of  $\pm 0.03$  K (Eppley Laboratory Inc. 1997). Data were logged to a computer via a controller unit, which allows the user to set the blackbody to a specific temperature to  $\pm 0.1$  K. A Campbell Scientific CR10X datalogger was used to log the output from two four-wire PRT units mounted within the CASOTS water bath, which had been end-to-end calibrated to an accuracy of better than  $\pm 0.05$  K. In this configuration the PRT sensors were logged at a resolution of  $\pm 0.01$  K.

Radiometer temperatures were obtained over a temperature range of 283–313 K in a constant-temperature room at  $295 \pm 0.5$  K. Each blackbody was given sufficient time to stabilize after any temperature changes had been made. As the emissivity for each cavity is different, a correction for the nonblackness was applied to the radiometer data based on regular radiometric measurements of the surrounding environment using the following equation:

$$R_{\text{true}} = \frac{[R_{\text{BB}} - (1.0 - \epsilon)R_{\text{env}}]}{\epsilon}, \quad (4)$$

where  $R_{\text{true}}$  is the true radiance leaving the cavity,  $R_{\text{BB}}$  is the radiance measured by the BB view radiometer and  $R_{\text{env}}$  is the mean radiance measured by the radiometer viewing the surrounding environment, and  $\epsilon$  is the effective emissivity of the appropriate BB. The radiometers are assumed to be stable during the measurement interval of 10 s to an accuracy of  $\pm 0.1$  K logged to a precision of  $\pm 0.01$  K.

Figure 6 shows the blackbody temperature plotted as a function of the difference between the BB temperature derived from the TASCOTHI-500L radiometer measurements and the temperature reported by the Eppley BB25TB (squares) and CASOTS BB (triangles). The magnitude of the differences between the two blackbody

systems are at the limit of the radiometer accuracy and clearly demonstrate the similarity between the two blackbody systems. Note that the linear trend with respect to the BB temperatures is a calibration error from the TASCOTHI radiometer, typical of these particular instruments.

#### d. Comparison between a CASOTS BB and an NIST water bath blackbody

During 5–6 March 1998, the Rosenstiel School of Marine and Atmospheric Science (RSMAS) and Centre for Earth Observation Science (CEOS) hosted an international infrared validation workshop aimed to provide a forum in which the various groups involved in the validation of satellite measurements of sea surface temperature could coordinate their activities. During this workshop a Marine Atmospheric Emitted Radiance Interferometer (MAERI; Knuteson et al. 1997) was used to obtain calibrated radiant temperatures from both a CASOTS blackbody and a National Institute of Standards and Technology (NIST) blackbody (Fowler 1995).

The NIST reference BB is able to maintain a fixed radiant temperature using an actively controlled water bath system, and the data presented here were collected at 283 K. The temperature of the NIST BB was allowed to stabilize at 283 K before the MAERI began collecting data, and the NIST temperature readout was reset to begin data averaging. The readout temperature stability was at the millikelvins level throughout the data collection period, and an average temperature was recorded at the end of the data run and taken as representative of the entire data collection period ( $\sim 11.5$  h). The CASOTS BB water temperature was logged with an immersible 100- $\Omega$  PRT and an ASL F250 Mk2 AC resistance bridge. The PRT was calibrated to an accuracy of  $\pm 20$  mK. The MAERI test began with the CASOTS at about 293 K and continued overnight ( $\sim 20$  h) until the blackbody reached about 307 K where it achieved an approximate equilibrium temperature. The MAERI viewed each BB with an integration time of 200 s at intervals of 510 s. The time between views of the BB cavities was spent viewing the MAERI internal calibration blackbodies.

The MAERI performs all data processing in real time to the level of calibrated radiances, and radiances were converted to equivalent brightness temperature for both shortwave (2510–2515  $\text{cm}^{-1}$ ) and longwave (985–990  $\text{cm}^{-1}$ ) in a postprocessing step for comparison to the reference temperature. The CASOTS temperature closest in time to the center of the MAERI CASOTS view was used to provide the difference measurement. The results of this experiment expressed as difference temperatures (MAERI-NIST and MAERI-CASOTS BB) are presented in Table 1. In both the shortwave and longwave spectral regions used to view the BB units, the difference between the CASOTS and the NIST BB

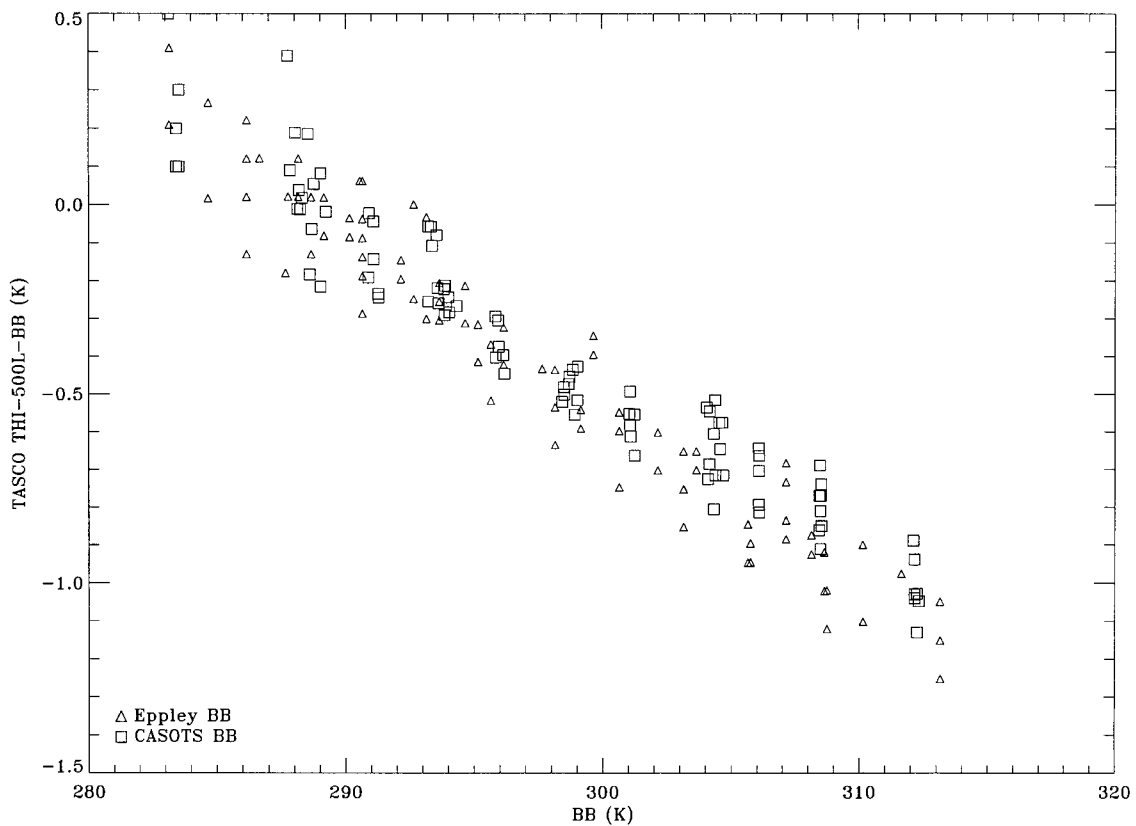


FIG. 6. CASOTS BB temperature plotted as a function of the difference between TASCO THI-500L radiometer brightness temperatures and the CASOTS BB radiant temperature (triangles) and Eppley BB radiant temperature (squares). During this experiment the CASOTS BB temperatures were measured by two PRT sensors to an accuracy of  $\pm 0.05$  K and precision of  $\pm 0.02$  K. The radiometer data have been corrected for the different emissivity differences of each BB cavity and have an accuracy of  $\pm 0.1$  K and a resolution of  $\pm 0.02$  K.

units is at the limit of the CASOTS PRT accuracy ( $\pm 20$  mK).

#### COMPARISON OF THE CASOTS BB USING A PRECISION INDEPENDENTLY CALIBRATED RADIOMETER

An alternative strategy to that described above is to use an accurate continuously calibrated radiometer to determine the temperature of the CASOTS BB over a range of typical operating temperatures. During the Chemical and Hydrographic Atlantic Ocean Survey (CHAOS) experiment in 1998 on the U.K. Natural En-

vironment Research Council vessel RRS *Discovery*, a CASOTS BB was used to calibrate a SISTeR radiometer.

Calibrations of the SISTeR against the CASOTS BB were made just before (23 April), part way through (11 May), and shortly after (12 June) the cruise, and Figs. 7a-c show the respective calibration residuals between the SISTeR and CASOTS BB. On each occasion, the CASOTS water bath was heated gently with an immersible fish tank heater and the water temperature was logged with an immersible 100- $\Omega$  PRT and an ASL F250 Mk2 AC resistance bridge. The PRT was calibrated to an accuracy of  $\pm 20$  mK. The SISTeR field of view was aligned with the center of the CASOTS BB aperture and the front face of the instrument was separated by 2 cm from that of the CASOTS BB. Measurements were made with the 10.8- $\mu\text{m}$  filter and each individual radiance sample taken by the SISTeR was integrated for 0.72 s. Mean calibration accuracies and standard deviations for a single radiance sample, generated from the complete calibration sequence, are included in the figures. A typical time profile for the temperatures of the CASOTS and SISTeR internal BBs, that for 23 April, is shown in Fig. 8.

TABLE 1. Results summary of a comparison between the CASOTS-003 and NIST blackbody derived from MAERI observations made at the RSMAS-CEOS workshop, University of Miami, Mar 1998. Results are for the MAERI minus the reference source temperatures.

Blackbody	Difference (K) at 985–990 $\text{cm}^{-1}$	Difference (K) at 2510–2515 $\text{cm}^{-1}$
CASOTS-003	0.024	0.014
NIST	0.013	0.010



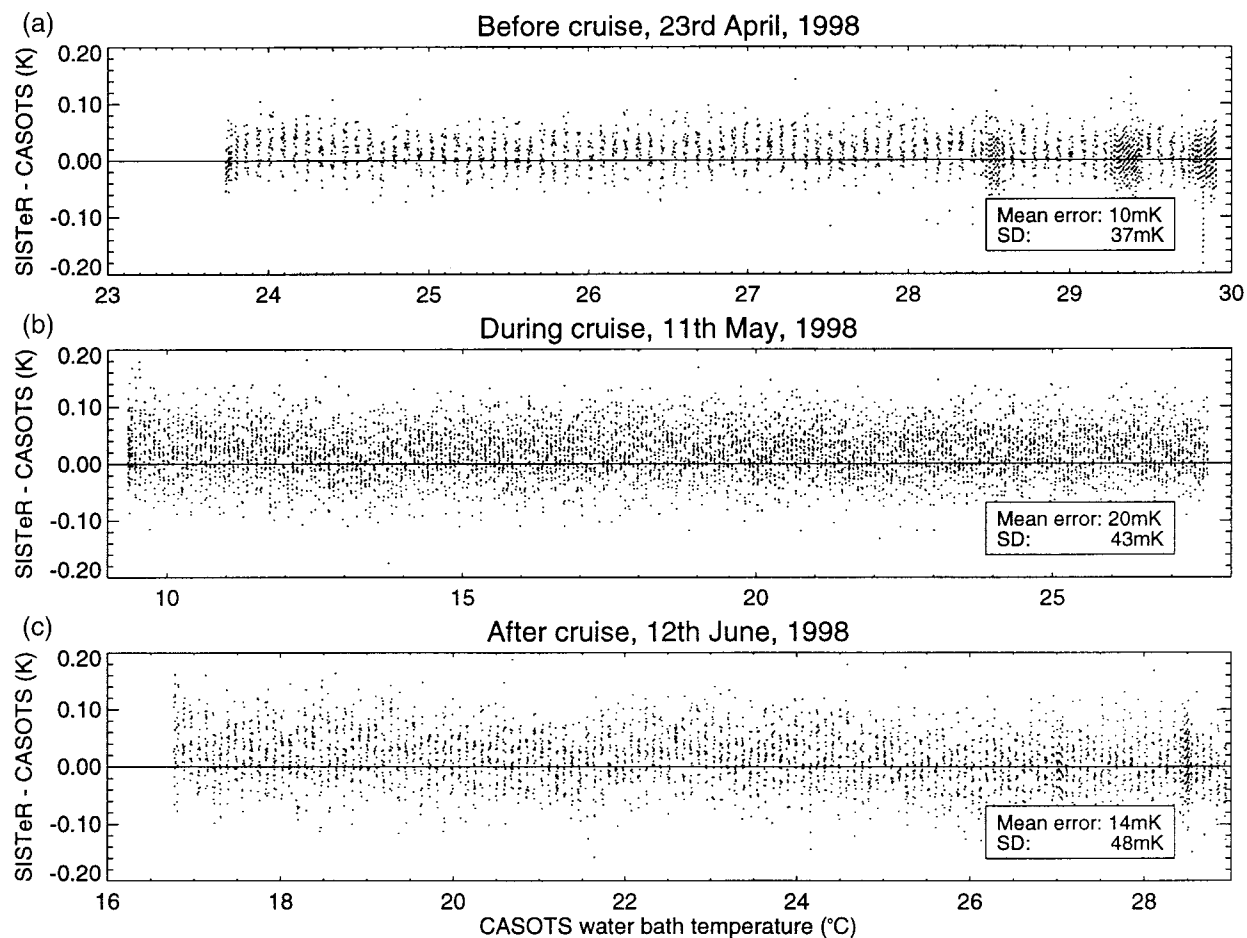


FIG. 7. Calibrations of the SISTeR radiometer against a CASOTS blackbody during the 1998 CHAOS experiment. The differences between the brightness temperature recorded by the SISTeR and the temperature of the CASOTS water bath are plotted as a function of water bath temperature for calibrations made (a) before, (b) during, and (c) after the cruise.

Owing to its exposed position at the bow of the RRS *Discovery*, the surface of the SISTeR's scan mirror degraded steadily throughout the cruise, due both to salt deposition and corrosion of the mirror substrate. Nonetheless, although the system noise increased as the mirror reflectivity fell, there was no significant change in the instrument calibration relative to the CASOTS BB. Indeed, the calibration accuracy was always within that of the PRT calibration and was repeatable to even higher accuracy. The consistency of the calibrations over the cruise period gave confidence in the stability of the SISTeR data.

A similar situation had occurred on the first SISTeR deployment (during the ROSSA/AMT-3 experiment) when it was considered prudent to replace the SISTeR scan mirror. The use of a CASOTS BB unit to obtain calibration data both before and after the mirror replacement was vital to assure continuity of the SISTeR dataset after the instrument had undergone such dramatic changes. These examples provide effective demonstrations of the intended application of the CASOTS BB.

#### e. Similarity of individual CASOTS BB units

To verify the degree of spectral similarity between a number of CASOTS BB, the brightness temperatures of three CASOTS BB were measured using a double-pendulum BOMEM MR-154 interferometer equipped with a liquid nitrogen cooled HgCdTe detector over a spectral range of 600 to 2000  $\text{cm}^{-1}$ . The interferometer was configured for a spectral measurement resolution of 1  $\text{cm}^{-1}$  and calibration was derived from two *ERS-1* along track scanning radiometer (ATSR) pre-flight calibration blackbodies (Mason et al. 1995) following the procedure of Revercomb et al. (1988). This technique uses the complex spectra of two calibration sources; in our case an ambient temperature ATSR blackbody is used as the cold source and a second, heated ATSR blackbody as the hot source. The temperature difference between the two ATSR blackbodies in this configuration was about 10 K. All spectra were obtained in a temperature-controlled room that was maintained at 293 K, and all blackbodies were positioned in front of the interferometer at a distance of 25 cm. No external mirror was used for

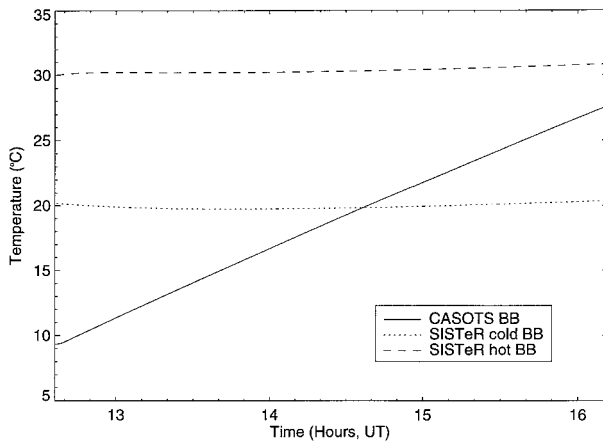


FIG. 8. CASOTS water bath and SISTeR internal blackbody temperatures from a calibration of the SISTeR radiometer against a CASOTS blackbody, recorded on 11 May during the 1998 CHAOS experiment.

this investigation. The interferometer had a relatively high temperature of 304 K, which resulted in an induced temperature drift of both ATSR blackbody units of approximately  $0.1 \text{ K min}^{-1}$  derived from six PRT units embedded within the ATSR BBs, which were calibrated to better than  $\pm 0.002 \text{ mK}$ . In order to minimize these

drifts, interferograms were computed by averaging over 40 independent scans. The temperatures recorded by several PRT sensors embedded within the ATSR blackbody units were contemporaneously recorded and then averaged over the same period as the interferometer calibration measurements. Spectral smoothing was undertaken using a running average having a spectral width of  $25 \text{ cm}^{-1}$  (Savitsky and Golay 1964).

Gases such as  $\text{CO}_2$  and  $\text{H}_2\text{O}$  present in the optical path between the blackbodies and the interferometer detector will have a significant influence outside the small spectral wave band of the infrared window ( $770\text{--}1100 \text{ cm}^{-1}$ ). However, within this wave band over small atmospheric path lengths, absorption and emission of such gases is minimal and comparisons between individual spectra are valid. To examine the spectral characteristics of the individual CASOTS BBs, the temperature difference between each CASOTS BB and the temperature of the interferometer has been used. The resulting spectra obtained from three CASOTS BB units is shown in Fig. 9. Interferometric measurements were made for each individual CASOTS BB, which were maintained at slightly different temperatures to each other (all  $\sim 294 \text{ K}$ ), resulting in a real  $\sim 0.75 \text{ K}$  offset between the individual spectra shown. The influence of atmospheric absorption and emission is clearly seen above and below

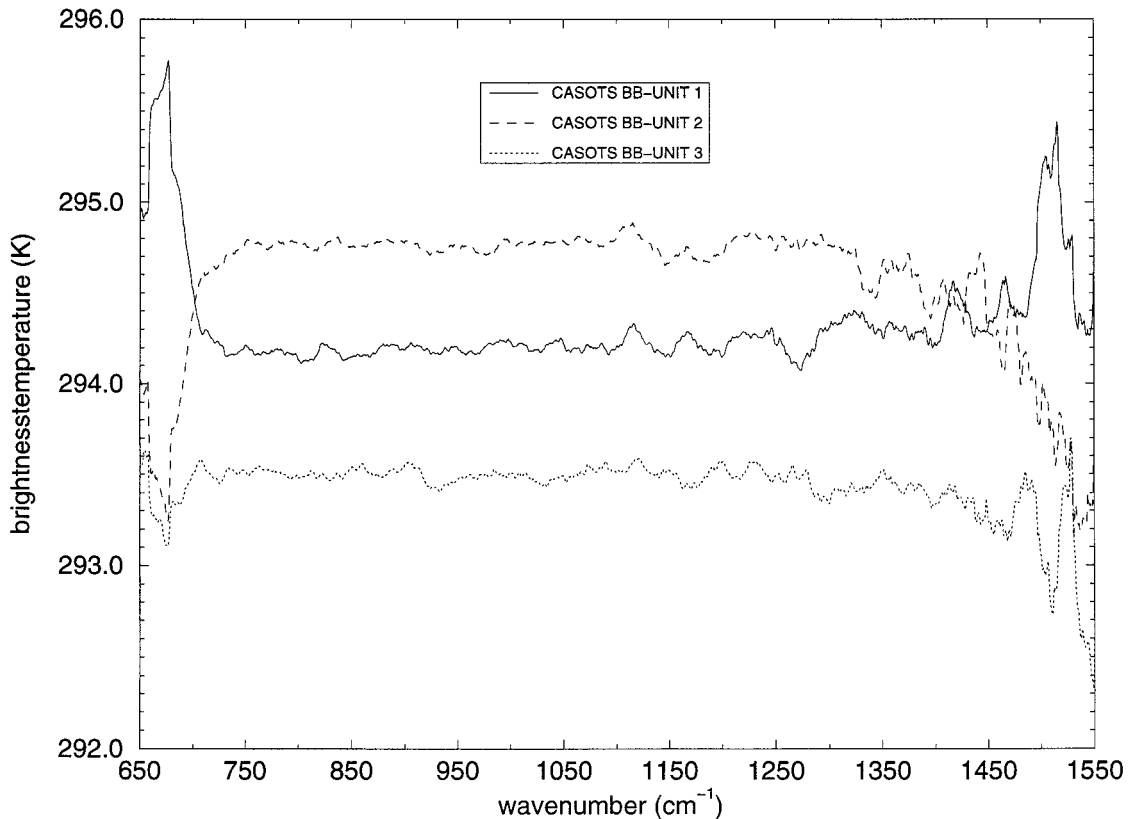


FIG. 9. Spectral comparison of three CASOTS blackbody units (CASOTS-001, CASOTS-002, and CASOTS-003) measured by a double-pendulum BOMEM MR-154 interferometer during the CASOTS 1996 radiometer intercalibration experiment.

TABLE 2. Summary of CASOTS blackbody characteristics.

Error type	Magnitude, K
PTR calibration	Better than 0.05 K
Emissivity calculation	0.01
Spatial gradients	0.1 K m <sup>-1</sup> at spot radii <30 mm
Temporal gradients	<0.02 K min <sup>-1</sup> at $\Delta T = \pm 10$ K

770 and 1100 wavenumber, which depends both on the temperature of the gases in the optical path and on the blackbody temperature itself. Note that the data obtained for CASOTS-001 were obtained on a different day from those shown for CASOTS-002 and -003 when different atmospheric conditions prevailed in the laboratory. However, within the region of 770–1100 wavenumber the spectra of the CASOTS BB are very similar and no significant difference between the three CASOTS BB units tested in this experiment can be recognized.

#### 4. Discussion of the CASOTS BB

Geist and Fowler (1986) suggest that the best way to determine the quality of a blackbody cavity is to over-design the cavity so that a simple worst case estimate can be used to determine the maximum deviation from ideal blackbody behavior. They describe a set of equations that account for thermal losses within their system and characterize the “quality” of their blackbody design. However, they acknowledge that it is extremely difficult to determine the exact radiative transfer properties of the cavity wall and surface finish because a truly rigorous theoretical analysis of the cavity quality is extremely complicated. In our case the use of modern thermal imagery and direct comparison with measurements derived from precision radiometers viewing independent blackbodies allow a thorough validation of the CASOTS BB to be presented.

Table 2 presents the significant error characteristics of the CASOTS BB expressed as temperatures. In agreement with Geist and Fowler (1986), the main source of error in the design is the accurate end-to-end calibration of the water bath temperature measurement system. There are a wide variety of sensors and logging systems available that are able to measure the temperature of the water bath to accuracies better than  $\pm 0.05$  K, and we use this figure as a nominal lower limit to the error budget of the CASOTS BB.

The accurate positioning of a radiometer in front of the CASOTS BB is important especially for radiometers having strongly divergent fields of view ( $>10^\circ$ ). To accurately position a radiometer in front of the CASOTS BB aperture we recommend that the CASOTS BB be held at a temperature significantly different from ambient and that a radiometer be “profiled” in both the horizontal and vertical direction to determine the “thermal center” of the CASOTS BB. In this way the optimum position for the radiometer in front of the blackbody can be derived based on the stability of the tem-

perature readings obtained during the profiling exercise. As an approximate guide to the maximum distance between the radiometer beam focus and the CASOTS BB aperture, assuming an upper limit of a 40-mm spot radius and a radiometer divergent beam of  $15^\circ$  (full width), the beam focus will be approximately 100 mm from the CASOTS BB aperture.

As the CASOTS BB  $\epsilon$  value is not unity, a small radiance contribution will form a component of the measured radiometer temperature due to direct reflection of the surrounding environmental radiance as shown by Eq. (4). The magnitude of this contribution will depend on the surrounding thermal conditions and will be greatest for radiometers having a large spot radius, reiterating that for the most accurate calibrations, the radiometer field of view should not exceed a spot radius of 40 mm. Typically, the temperature of the area surrounding the CASOTS BB is more difficult to control in the field than in the laboratory (where temperature-controlled rooms may be used) because in the field multiple radiant sources are often present such as people, windows, open sky views, etc. Thus, the accuracy of the CASOTS BB will be slightly reduced if the external radiance sources remain unaccounted for (Richardson 1991) especially when these are significantly different or variable in comparison to the CASOTS BB. To ensure the highest calibration accuracy possible we recommend that the surrounding area should be maintained at near isothermal conditions similar to the actual CASOTS BB temperature.

During initial calibration experiments we found that condensation was prone to form at the cavity aperture once the dewpoint temperature of the surrounding air had been reached. At temperatures below this, the entire BB cavity became visibly wet. Although the emissivity of water (also a diffuse reflector) is higher ( $\epsilon_{\text{water}} \sim 0.99$ ) than that of the Nextel paint ( $\epsilon_{\text{Nextel}} = 0.96$ ) used to coat the cavity walls, a strong temperature gradient can be supported by the water surface, which is primarily related to the heat flux passing through it. When large differences between air temperature and CASOTS BB temperature prevail, a “skin” temperature deviation will be maintained in the condensate covering the CASOTS BB that will significantly decouple the radiative temperature of the CASOTS BB measured by a radiometer from the water bath temperature, which is measured by PRT units. Consequently, any measurements made in such conditions must be treated with extreme caution. To avoid this situation, the cavity temperature should not be allowed to fall below the local dewpoint temperature. Only in a dry (nitrogen or helium purged) atmosphere should the lower range of temperature (e.g.,  $< 273$ – $278$  K) be set.

#### 5. CASOTS radiometer intercalibration experiment

Many different in situ infrared radiometers, spectroradiometers, and thermal imaging cameras are now be-

ing used to collect precision in situ SSST datasets. Some instruments feature robust onboard calibration systems while others rely on solid state electronics or external calibration targets to maintain instrument calibration. When these instruments are subject to significant variations in atmospheric temperature, humidity, and direct warming by solar radiation, significant calibration errors may occur. Additional calibration uncertainties can be caused by the datalogging system itself through the effects of uncompensated long cables or drifts in the electronics packages affecting analog to digital conversion. Many instruments use different spectral wave bands to determine SSST, requiring careful consideration of the most appropriate target emissivity value. Finally, there is limited formal agreement on a set of protocols for the measurement of SSST using in situ radiometer systems. One of the major themes within the CASOTS project was to promote the exchange of practical experience and information on skin temperature measurements, techniques, problems, and solutions. The development of the CASOTS blackbody units together with the implementation of a radiometer intercalibration experiment were direct responses to this remit. Only by conducting detailed calibration and intercomparison experiments can field radiometers be used with any degree of confidence. Using a relative reference standard such as the CASOTS blackbody unit described here, field observations made by different research groups using different radiometer instruments can be standardized. Such a coordinated approach to radiometer calibration is vital for the successful measurement of SSST, for the ongoing global validation of satellite derived SSST observations, and for the development of techniques and algorithms that comprehensively describe the ocean SSST.

#### *a. Methods of radiometer intercalibration*

The calibration of an infrared radiometer system can be defined as quantitatively defining a radiometer system response to accurately defined and controlled system inputs [Eq. (1)]. Of paramount importance is the need to calibrate the entire instrument system for a range of both target and instrument temperatures. Many instrument detector elements respond to changes in ambient temperature so that changing instrument temperatures will cause changes in any stray radiation emitted from within a radiometer falling onto the detector element (e.g., Thomas et al. 1995). This effect needs to be adequately addressed in any radiometer calibration or intercomparison exercise by varying the instrument temperature when viewing a well-characterized radiance target.

There are several possibilities to consider as potential calibration targets, which include viewing the sea surface itself, the surface of a well-stirred water bath, or a blackbody cavity. When viewing the sea surface it is

difficult to reliably control the radiative characteristics for a number of reasons:

- It is difficult to maintain consistent surface roughness except in extremely calm wind regimes. These are also the conditions when the BSST–SSST difference is highly variable.
- It is difficult to accurately determine the radiative temperature of the sea surface using in situ temperature sensors, due to the BSST–SSST difference.
- It is difficult to assure that the surface water remains completely uncontaminated by surfactants that may significantly modify the surface emissivity characteristics. This is especially true close to the shoreside or jetties where contamination is prone to occur.
- It is difficult to maintain consistent sky conditions and environmental conditions (air temperature, solar radiation, humidity) for the typical duration of an intercalibration exercise.
- Poor weather conditions may prevent the experiment from taking place.

In the case of a stirred water bath, it is difficult to assure complete mixing of the water bath (and hence prevent a BSST–SSST difference) and consistent surface roughness characteristics, due to the inevitable water bulge that results from vigorous stirring of the water as discussed in section 2. We consider that the best solution is to use a well-defined temperature-controlled cavity blackbody in a temperature-controlled chamber. The advantage of this combination is that it provides the maximum control over the calibration system inputs during the calibration exercise, ultimately facilitating the comparison of several different radiometer systems.

#### *b. Experiment procedure and results*

The main objective of the CASOTS radiometer intercalibration experiment was to quantify both the relative and absolute calibration of several narrowband, small field-of-view infrared radiometer systems currently used to determine SSST by research groups from around the world. Table 3 describes the main characteristics of the radiometer systems that participated in the experiment, which was undertaken at the Southampton Oceanography Centre, Southampton, United Kingdom, during 17–21 June 1996. Most of the participating instruments were single-channel radiometers relying on some form of internal temperature compensation circuitry or a single reference black body to maintain a stable calibration. However several more sophisticated instruments used two internal blackbody calibration cavities.

In order to quantify any systematic calibration bias due to instrument warming and to quantify the mean difference between all radiometers, three temperature-regulated environmental chambers were used. The chambers were set and maintained at temperatures of 278 (cold), 293 (ambient), and 303 K (hot) to simulate



TABLE 3. The main characteristics of the infrared radiometer instruments participating in the first CASOTS radiometer intercalibration experiment.

Instrument	Wave band	Channels	Calibration method	No.
SIL STR-100	10.5–12.5	2	3 Internal BB	1
TASCO THI-500L	8.0–12.0	1	Solid state	4
Hiemann KT-19	8.0–10.0	1	1 Internal BB	1
Hiemann KT-15	8.0–10.0	1	1 Internal BB	1
Exergen IRt/c	6.5–14.0	2	Solid state	2
Everest 4000	8.0–13.0	1	Solid state	1
RAL SISTeR	10.8	1	3 Internal BB	1

the typical air temperatures of the subpolar to tropical regions. Two CASOTS BB systems were used, and for the purpose of this exercise water bath temperatures were logged using two 100-Ω PRT sensors connected to Campbell Scientific CR10 datalogger system. The PRT units were calibrated to an accuracy of better than ±0.05 K and were logged to a precision of ±0.01 K. Each radiometer system viewed a CASOTS BB over a

temperature range of 283–308 K in each of the temperature rooms described above. The atmospheric conditions prevalent during the experiment meant that the dewpoint temperature would be reached at temperatures below 283 K. Thus, every attempt was made to prevent condensation occurring during the experiment, which included limiting the lower range of CASOTS BB temperatures. Measurements commenced after individual radiometer systems had been allowed sufficient time to thermally stabilize at the environment room temperature, which was typically about 2–3 h. A minimum of four data points were obtained for each instrument for all three chamber temperatures.

Figure 10 plots the CASOTS BB temperature as a function of the residual difference between the radiometer measurements and CASOTS BB temperature for each of the instruments described in Table 3. To aid interpretation, the data from each radiometer system have been plotted using identical colors for the cold (crosses), ambient (asterisk), and hot (diamond) chamber temperatures. In some cases, large systematic biases

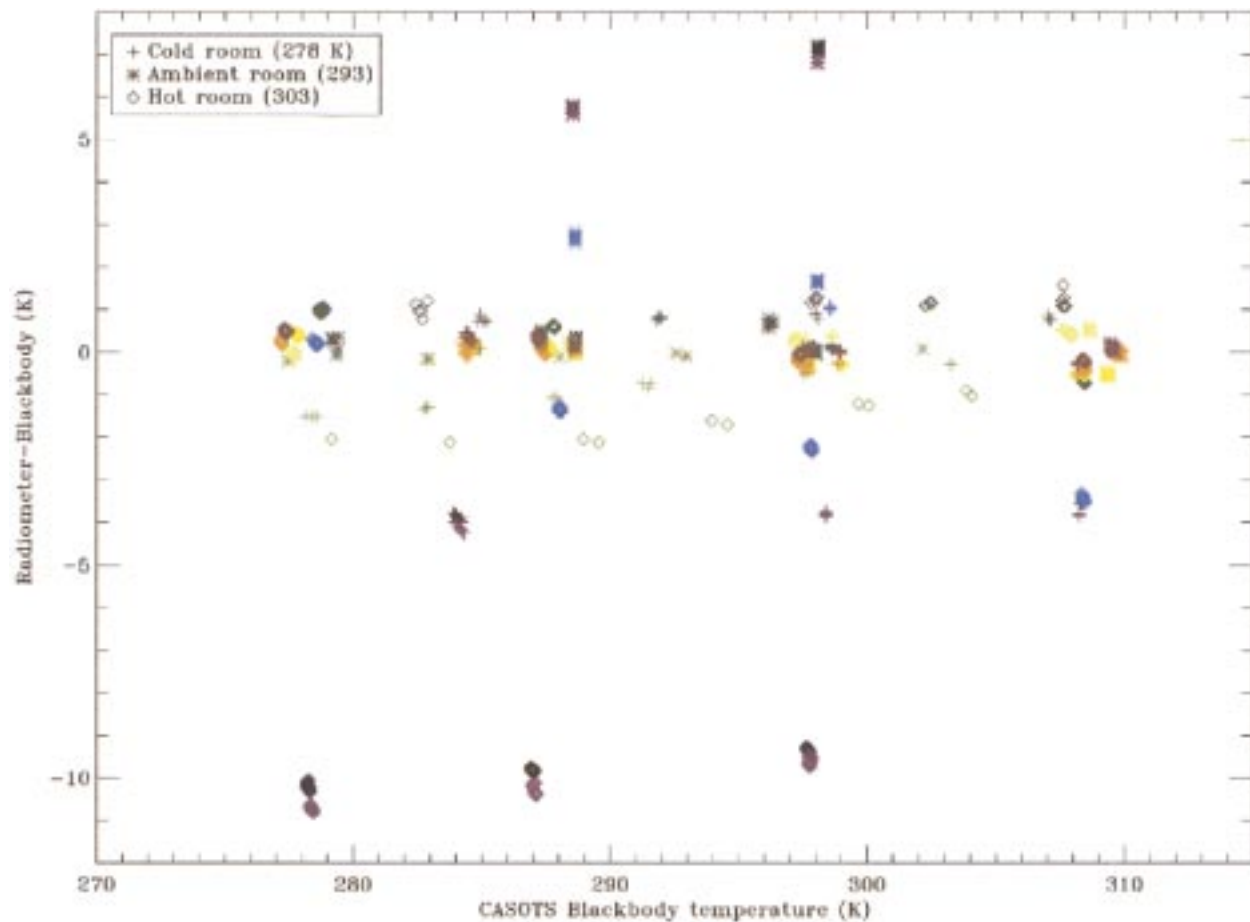


FIG. 10. CASOTS BB temperature plotted as a function of the difference between the brightness temperature recorded by each of the radiometers described in Table 3 and CASOTS BB temperature. All of the data obtained by a specific radiometer are shown in the same color, and the symbols used refer to the particular chamber temperature. Data were obtained during the CASOTS 1996 radiometer intercalibration experiment.

in excess of 5 K exist associated with the extreme hot and cold environment conditions. However, in most cases, the calibration data demonstrate that the radiometers are accurate to within  $\pm 3$  K. The degree of scatter shown in Fig. 10 suggests one reason for the difficulty in reconciling many published sea surface skin temperature observations with each other since many are distinctly different in character. Clearly such differences are unacceptable for the investigation of the SSST or the validation of satellite-derived SSST data and highlight the need for further experiments of this type.

## 6. Conclusions

A water bath blackbody calibration radiance source that is suitable for the accurate calibration of sea-going infrared radiometers has been designed and built. The blackbody is suitable for use both in the field and laboratory and consists of a circular 100-mm diameter cavity painted with high emissivity paint and immersed in a water bath. Thermal imagery shows the cavity to be isothermal for radiometer spot radii of up to 40 mm centered on the BB cavity apex. Due to temperature gradients concentrated at the lip of the cavity, instruments should be carefully set to view only the deepest inner part of the cavity. The temporal stability of the CASOTS BB is  $0.02 \text{ K min}^{-1}$  and analysis of three identical units shows that spectral differences are negligible in the spectral region of  $770$  to  $1100 \text{ cm}^{-1}$ . Validation data using independently calibrated radiance measurements and an NIST standard and a commercial blackbody unit show that the CASOTS blackbody is a reliable radiance source accurate to better than  $\pm 0.02$  K. The controlling factor defining the accuracy of this design is the stability and calibration of the the water bath temperature measurement.

Several example field deployments of the CASOTS BB are used to demonstrate the need to provide a robust, accurate, and portable calibration standard for use while at sea. Our results suggest that it is essential to provide independent calibration data before any radiometer field measurements can be treated with confidence. The benefit of developing a portable blackbody system, which can be used in the field, is that it removes much of the uncertainty associated with significant instrument modification or contamination. Data obtained during the CASOTS radiometer intercalibration experiment clearly show that large calibration uncertainties exist for several individual radiometer instruments, which can be accounted for by obtaining independent calibration data to standardize the measurements. These data highlight the need for regular relative calibration exercises using independent blackbody systems to standardize different radiometer instrument calibrations. Only through the regular intercomparison and calibration of field radiometer instruments can measurements of the sea surface skin temperature be improved and much of the uncertainty associated with such measurements be accounted

for. Such data are vital for the development of improved parameterizations for the bulk skin temperature difference and the accurate international global validation of satellite-derived sea surface skin temperatures.

*Acknowledgments.* The authors would like to acknowledge the support of colleagues at the Southampton Oceanography Centre in the use of laboratories, especially R. Pascall and G. Griffiths. We would like to thank the Rutherford Appleton Laboratory and I. Mason for the use of the along-track scanning radiometer blackbody units; Fred Best and Bob Knuteson for the MAERI results collected at the RSMAS-CEOS intercalibration exercise; I. Barton, S. Keogh, I. Ridley, B. Ward, and E. de Jong for their contributions to the CASOTS radiometer intercalibration experiment; T. Sheasby for providing the CHAOS calibration datasets; Andy Jessup of the Applied Physics Laboratory, University of Washington, for the Amber thermal camera images; and Joe Shaw of NOAA/Environmental and Technology Division, Boulder, Colorado, for the use of the Eppley blackbody units. This work was partly funded by NASA Grant NAGW-1110 and the EC Framework 4 Environment and Climate Programme Contract ENV4-CT95-0149.

## REFERENCES

- Bell, P. A., 1995: Evaluation of temporal stability and spatial uniformity of blackbody thermal reference sources. *SPIE*, **2470**, 300–311.
- Berry, K. H., 1981: Emissivity of a cylindrical blackbody cavity with a re-entrant cone end face. *J. Phys. E: Sci. Instr.*, **14**, 629–632.
- Betts, D. B., F. J. J. Clarke, L. J. Cox, and J. A. Larkin, 1985: Infrared reflection properties of five types of black coating for radiometric detectors. *J. Phys. E: Sci. Instr.*, **18**, 689–696.
- Donlon, C. J., 1997: Radiometric observations of the sea surface and atmosphere. 1996 Cruise Rep., 15 pp. [Available from Colorado Center for Astrodynamic Research, University of Colorado at Boulder, Boulder, CO 80309-0429.]
- , and I. S. Robinson, 1997: Observations of the oceanic thermal skin in the Atlantic Ocean. *J. Geophys. Res.*, **102**, 18 585–18 606.
- , and —, 1998: Radiometric validation of the *ERS-1* ATSR average sea surface temperature in the Atlantic Ocean. *J. Atmos. Oceanic Technol.*, **15**, 647–660.
- Eppley Laboratory Inc., 1997: Operation and instructions manual for blackbody calibration source model BB25TB. Rep. S/N 10194. [Available from Eppley Laboratory Inc., 12 Sheffield Ave., P.O. Box 419, Newport, RI 02840.]
- Fiedler, L., and S. Bakan, 1997: Interferometric measurements of sea surface temperature and emissivity. Max-Planck-Institut für Meteorologie Rep. 232, 16 pp. [Available from Max-Planck-Institut für Meteorologie, Bundesstrasse 55, Hamburg 20146, Germany.]
- Fowler, J. B., 1995: A third generation water bath based blackbody source. *J. Res. NIST*, **100**, 591.
- Geist, J., and J. B. Fowler, 1986: A water bath blackbody for the 5 to 60 degree temperature range: Performance goals, design concept, and test results. U.S. National Bureau of Standards Tech. Note 1228, 16 pp. [Available from National Bureau of Standards, Gaithersburg, MD 20899.]
- Grassl, H., and H. Hinzpeter, 1975: The cool skin of the ocean. WMO GATE Rep. 14.
- Kent, E. T., T. Forrester, and P. K. Taylor, 1996: A comparison of the

- oceanic skin effect parameterizations using ship-borne radiometer data. *J. Geophys. Res.*, **101**, 16 649–16 666.
- Knuteson, R. O., F. A. Best, H. B. Howell, P. Minnett, H. E. Revercomb, and W. L. Smith, 1997: High spectral resolution infrared observations at the ocean–atmosphere interface in the tropical western Pacific using a Marine Atmospheric Emitted Radiance Interferometer (MAERI): Applications to SST validation and atmospheric spectroscopy. Preprints, *Ninth Conf. on Atmospheric Radiation*, Long Beach, CA, Amer. Meteor. Soc., 180–183.
- Lohrengel, R., and R. Todtenhaupt, 1996: Wärmeleitfähigkeit, Gestamtemissionsgrade und spektrale Emissionsgrade der Beschichtung Nextel-Velvet-Coating 811-211 (RAL 900 15 teifschwartz matt). *PTB-Mitteilungen*, **106**, 259–265.
- Mason, I., M., P. H. Sheather, J. A. Bowles, and G. Davies, 1995: Blackbody calibration sources of high accuracy for a space-borne infrared instruments—The along track scanning radiometer. *Appl. Opt.*, **35** (4), 629–639.
- Nightingale, T. J., 1992: Investigation of the radiometric performance of the improved stratospheric and mesospheric sounder. Ph.D. thesis, University of Oxford, 201 pp. [Available from Space Science Department, Rutherford Appleton Laboratory, Chilton, Didcot, Oxford OX11 0QX, United Kingdom.]
- Revercomb, H. E., H. Buijs, H. B. Howell, D. D. Laporte, W. L. Smith, and L. A. Sromovsky, 1988: Radiometric calibration of IR Fourier transform spectrometers: Solution to a problem with the high resolution interferometer sounder. *Appl. Opt.*, **27**, 3210–3218.
- Richardson, I., 1991: Radiometric vs. thermometric calibration of IR test systems: Which is best? *SPIE*, **1488**, 80–88.
- Saurez, M., W. J. Emery, and G. Wick, 1997: The Multi-Channel Infrared Sea Truth Radiometric Calibrator (MISTRIC). *J. Atmos. Oceanic Technol.*, **14**, 243–253.
- Savitzky, A., and M. J. E. Golay, 1964: Smoothing and differentiation of data by simplified least squares procedures. *Analyt. Chem.*, **36**, 1627–1639.
- Schlüssel, P., H. Y. Shin, W. J. Emery, and H. Grassl, 1987: Comparison of satellite derived sea surface temperatures with in situ skin measurements. *J. Geophys. Res.*, **92**, 2859–2874.
- , W. J. Emery, H. Grassl, and T. Mammen, 1990: On the bulk skin temperature difference and its impact on satellite remote sensing of sea surface temperature. *J. Geophys. Res.*, **95**, 13 341–13 356.
- Siegel, R., and J. R. Howell, 1981: *Thermal Radiation Heat Transfer*. 2d ed. McGraw Hill, 107 pp.
- Smith, A. H., R. W. Saunders, and A. M. Závody, 1994: The validation of ATSR using aircraft radiometer data over the tropical Atlantic. *J. Atmos. Oceanic Technol.*, **11**, 789–800.
- Tanba, S., S. Oikawa, R. Yokoyama, I. Ridley, I. Parkes, and D. Llewellyn-Jones, 1997: The relationship between SST measured from ATSR to the spatial and temporal behavior of ocean skin temperature as observed with an in situ thermal infrared camera. *Proc. Third ERS Symp.*, Florence, Italy, European Space Agency.
- Thomas, J. P., and J. Turner, 1995: Validation of Atlantic Ocean surface temperatures measured by the *ERS-1* along track scanning radiometer. *J. Atmos. Oceanic Technol.*, **12**, 1303–1312.
- , R. J. Knight, H. K. Roscoe, J. Turner, and C. Symon, 1995: An evaluation of a self-calibrating infrared radiometer for measuring sea surface temperature. *J. Atmos. Oceanic Technol.*, **12**, 301–316.
- Zappa, C. J., 1997: Test of OPHIR calibration bucket using infrared imagery. University of Washington Internal Rep., 12 pp. [Available from the Applied Physics Laboratory, University of Washington, Seattle, WA 98105.]